A Sensitive Technique Using Atomic Force Microscopy to Measure the Low Earth Orbit Atomic Oxygen Erosion of Polymers

Kim K. de Groh and Bruce A. Banks
Glenn Research Center, Cleveland, Ohio

Gregory W. Clark
Manchester College, North Manchester, Indiana

Anne M. Hammerstrom, Erica E. Youngstrom, Carolyn Kaminski,
Elizabeth S. Fine, and Laura M. Marx
Hathaway Brown School, Shaker Heights, Ohio

December 2001

The NASA STI Program Office . . . in Profile

Since its founding, NASA has been dedicated to the advancement of aeronautics and space science. The NASA Scientific and Technical Information (STI) Program Office plays a key part in helping NASA maintain this important role.

The NASA STI Program Office is operated by Langley Research Center, the Lead Center for NASA's scientific and technical information. The NASA STI Program Office provides access to the NASA STI Database, the largest collection of aeronautical and space science STI in the world. The Program Office is also NASA's institutional mechanism for disseminating the results of its research and development activities. These results are published by NASA in the NASA STI Report Series, which includes the following report types:

- TECHNICAL PUBLICATION. Reports of completed research or a major significant phase of research that present the results of NASA programs and include extensive data or theoretical analysis. Includes compilations of significant scientific and technical data and information deemed to be of continuing reference value. NASA's counterpart of peer-reviewed formal professional papers but has less stringent limitations on manuscript length and extent of graphic presentations.

- TECHNICAL MEMORANDUM. Scientific and technical findings that are preliminary or of specialized interest, e.g., quick release reports, working papers, and bibliographies that contain minimal annotation. Does not contain extensive analysis.

- CONTRACTOR REPORT. Scientific and technical findings by NASA-sponsored contractors and grantees.

- CONFERENCE PUBLICATION. Collected papers from scientific and technical conferences, symposia, seminars, or other meetings sponsored or cosponsored by NASA.

- SPECIAL PUBLICATION. Scientific, technical, or historical information from NASA programs, projects, and missions, often concerned with subjects having substantial public interest.

- TECHNICAL TRANSLATION. English-language translations of foreign scientific and technical material pertinent to NASA's mission.

Specialized services that complement the STI Program Office's diverse offerings include creating custom thesauri, building customized data bases, organizing and publishing research results . . . even providing videos.

For more information about the NASA STI Program Office, see the following:

- Access the NASA STI Program Home Page at *http://www.sti.nasa.gov*

- E-mail your question via the Internet to help@sti.nasa.gov

- Fax your question to the NASA Access Help Desk at 301–621–0134

- Telephone the NASA Access Help Desk at 301–621–0390

- Write to:
  NASA Access Help Desk
  NASA Center for AeroSpace Information
  7121 Standard Drive
  Hanover, MD 21076
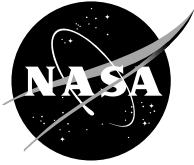
A Sensitive Technique Using Atomic Force Microscopy to Measure the Low Earth Orbit Atomic Oxygen Erosion of Polymers

Kim K. de Groh and Bruce A. Banks
Glenn Research Center, Cleveland, Ohio

Gregory W. Clark
Manchester College, North Manchester, Indiana

Anne M. Hammerstrom, Erica E. Youngstrom, Carolyn Kaminski,
Elizabeth S. Fine, and Laura M. Marx
Hathaway Brown School, Shaker Heights, Ohio

National Aeronautics and
Space Administration

Glenn Research Center

December 2001

A Sensitive Technique Using Atomic Force Microscopy to Measure the Low Earth Orbit Atomic Oxygen Erosion of Polymers

Kim K. de Groh
Bruce A. Banks
NASA Glenn Research Center, Cleveland Ohio 44135

Gregory W. Clark
Manchester College, North Manchester, Indiana 46962

Anne M. Hammerstrom, Erica E. Youngstrom, Carolyn Kaminski,
Elizabeth S. Fine and Laura M. Marx
Hathaway Brown School, Shaker Heights, Ohio 44122

Abstract

Polymers such as polyimide Kapton and Teflon FEP (fluorinated ethylene propylene) are commonly used spacecraft materials due to their desirable properties such as flexibility, low density, and in the case of FEP low solar absorptance and high thermal emittance. Polymers on the exterior of spacecraft in the low Earth orbit (LEO) environment are exposed to energetic atomic oxygen. Atomic oxygen erosion of polymers occurs in LEO and is a threat to spacecraft durability. It is therefore important to understand the atomic oxygen erosion yield (E, the volume loss per incident oxygen atom) of polymers being considered in spacecraft design. Because long-term space exposure data is rare and very costly, short-term exposures such as on the shuttle are often relied upon for atomic oxygen erosion determination. The most common technique for determining E is through mass loss measurements. For limited duration exposure experiments, such as shuttle experiments, the atomic oxygen fluence is often so small that mass loss measurements can not produce acceptable uncertainties. Therefore, a recession measurement technique has been developed using selective protection of polymer samples, combined with post-flight atomic force microscopy (AFM) analysis, to obtain accurate erosion yields of polymers exposed to low atomic oxygen fluences. This paper discusses the procedures used for this recession depth technique along with relevant characterization issues. In particular, a polymer is salt-sprayed prior to flight, then the salt is washed off post-flight and AFM is used to determine the erosion depth from the protected plateau. A small sample was salt-sprayed for AFM erosion depth analysis and flown as part of the Limited Duration Candidate Exposure (LDCE-4,-5) shuttle flight experiment on STS-51. This sample was used to study issues such as use of contact versus non-contact mode imaging for determining recession depth measurements. Error analyses were conducted and the percent probable error in the erosion yield when obtained by the mass loss and recession depth techniques has been compared. The recession depth technique is planned to be used to determine the erosion yield of 42 different polymers in the shuttle flight experiment PEACE (Polymer Erosion And Contamination Experiment) planned to fly in 2002 or 2003.

1. Introduction

Polymers such as polyimide Kapton and Teflon FEP (fluorinated ethylene propylene) are commonly used spacecraft materials due to their desirable properties such as flexibility, low density, electrical properties and in the case of FEP, a very low solar absorptance and high thermal emittance. A few examples of the use of polymers on the exterior of spacecraft include: back surface metallized Teflon FEP thermal control materials on the Hubble Space Telescope, polyimide Kapton solar array blankets (structural member) and Teflon ePTFE (expanded polytetrafluorethylene) cable insulation on the International Space Station.

Polymers on the exterior of spacecraft are exposed to atomic oxygen in the low Earth orbit (LEO) environment. Atomic oxygen is formed when short wavelength ultraviolet radiation (>5.12 eV, <243 nm) from the Sun dissociates molecular oxygen in the upper atmosphere.[1] Although atomic oxygen is the predominant species in LEO (below ≈1,000 km)[2], these neutral oxygen atoms have mean free paths on the order of 10^4 m at 400 km, resulting in extremely low probabilities of re-association. A typical LEO spacecraft orbits the Earth with a velocity on the order of 7.7 km/sec as it rams into the atmospheric oxygen (hence the term ram atomic oxygen). The flux of atomic oxygen at International Space Station (ISS) altitudes is approximately 1.0 x 10^{14} atoms/cm^2 sec for normal incident ram surfaces, and the average energy of an oxygen atom impacting spacecraft at ram velocities is 4.5 eV.[3] A number of processes can take place when an oxygen atom strikes a spacecraft surface at orbital velocities. These include chemical reaction with surface atoms or adsorbed molecules, elastic scattering, scattering with partial or full thermal accommodation, recombination, or excitation of ram species.[4] Because the oxidation product for most polymers is a gas, erosion results.

Atomic oxygen erosion of polymers in LEO is a serious threat to spacecraft durability. For example, depths of more than 0.0127 cm (0.005") thickness of Kapton and Mylar sheets were eroded away after 5.8 years in LEO on the leading edge, or ram atomic oxygen surface, of the Long Duration Exposure Facility (LDEF).[5] The atomic oxygen fluence for the leading edge of LDEF was 8.99 x 10^{21} atoms/cm^2.[6] In addition to the erosion of the Kapton and Mylar films, ≈1 ply (0.0127 cm or 0.005") of graphite-epoxy and 0.0025 cm (0.001") of Teflon FEP were also eroded away after 5.8 years on LDEF's leading edge.[5] Figure 1 shows a fluoropolymer (polychlorotrifluoroethylene) that was exposed to near normal incidence ram atomic oxygen on the leading edge of LDEF. A cone-like or carpet type morphology developed, which is characteristic of directed atomic oxygen erosion for materials with gaseous oxidation products. Protective coatings are effective in preventing atomic oxygen erosion, yet oxidation erosion of the underlying polymer can still occur at pinhole and scratch defects through atomic oxygen undercutting erosion.[7-9]

In addition to the obvious potential degradation to the structural ability of the polymers such as the support of solar cells on Kapton polyimide blankets on the International Space Station solar array, atomic oxygen is a threat to other materials properties. For example, the thermal emittance of thin polymer thermal control materials is dependent upon the thickness of the polymer. Thus erosion of the polymer by atomic oxygen can result in a reduced thermal emittance capability which would give rise to increases in the spacecraft temperature. It is therefore essential to

understand the atomic oxygen erosion yield (E, the volume loss per incident oxygen atom) of polymers being considered in spacecraft design. Procedures have been established for ground laboratory atomic oxygen interaction evaluation of materials for space applications.[10] Although ground laboratory procedures have been established and are used for erosion yield determination, actual in-space data is more reliable and therefore greatly more desired than ground tests. But, achieving the necessary levels of atomic oxygen fluence for many space experiments is a problem. Because long-term space exposure data, such as on the LDEF, is rare and very costly, short-term exposures such as on the shuttle have often been relied upon for atomic oxygen erosion determination. The most common technique for determining E is through mass loss measurements. For limited duration exposure experiments, such as shuttle flight experiments, the atomic oxygen fluence is often so small that mass loss measurements can not produce acceptable uncertainties. Therefore, a recession measurement technique has been developed at Glenn Research Center (GRC) over the past several years using intimate contact selective protection of polymer samples, combined with post-flight atomic force microscopy (AFM) analysis, to obtain accurate erosion yields of polymers exposed to low atomic oxygen fluences. Space flight samples protected in this manner have been recently used to help define AFM experimental procedures. This paper discusses in detail this recession measurement technique, the specific procedures used, along with numerous relevant characterization issues. Also conducted and reported in detail are error analyses for both the mass loss and recession depth techniques, which are compared with previously conducted analyses.
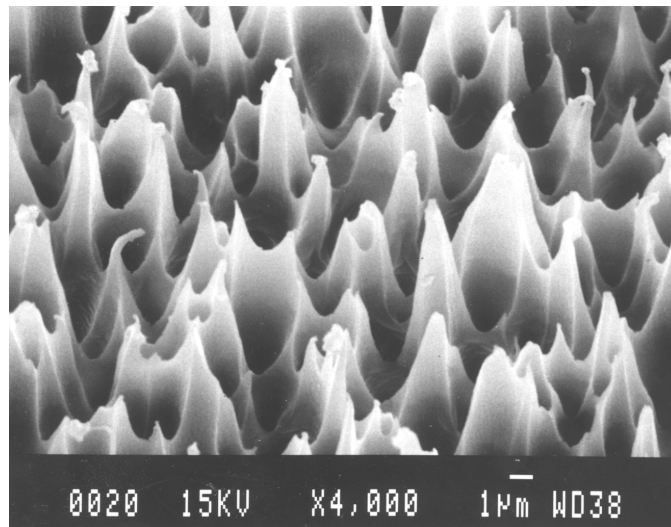

Figure 1. This fluoropolymer (polychlorotrifluoroethylene) was located on the leading edge of LDEF and shows the recession morphology which is typical of directed ram atomic oxygen erosion.

2. Erosion Yield Determination Techniques

2.1.   Mass Loss Measurements: Technique Issues and Problems for Short Duration Experiments.

The most common technique for determining the E of flight samples is through mass loss measurements. These measurements are made by obtaining mass measurements of the flight sample before and after flight. The erosion yield of the sample (E_S) is then calculated through the following equation:

$$E_S = \frac{\Delta M_S}{(A_S \rho_S F)}$$
(1)

where

E_s = erosion yield of the flight sample (cm³/atom)
ΔM_s = mass loss of the flight sample (g)
A_s = surface area of the flight sample exposed to atomic oxygen attack (cm²)
ρ_s = density of sample (g/cm³)
F = fluence of atomic oxygen (atoms/cm²)

The atomic oxygen fluence (F) can be characterized by determining the mass loss of a Kapton witness sample because Kapton has a well characterized erosion yield in the LEO environment, and can be calculated using the following equation:

$$F = \frac{\Delta M_K}{(A_K \rho_K E_K)}$$
(2)

where

ΔM_K = mass loss of Kapton witness sample (g)
A_K = surface area of Kapton witness sample exposed to atomic oxygen
ρ_K = density of Kapton witness sample (1.42 g/cm³)
E_K = erosion yield of Kapton witness sample (3.0 x 10⁻²⁴ cm³/atom)

Thus

$$E_S = E_K \frac{\Delta M_S A_K \rho_K}{\Delta M_K A_S \rho_S}$$
(3)

2.1.1. Rehydration/Dehydration Issues.   One of the critical issues with obtaining accurate erosion yield data from mass measurements is making sure that dehydrated mass measurements are used. Many polymer materials, such as Kapton, are very hygroscopic and therefore their mass can fluctuate significantly with humidity and temperature. Therefore, for accurate mass loss measurements to be obtained, it is necessary that the samples are fully dehydrated (in a vacuum desiccator, for example) prior to measuring the mass for both the pre-flight and post-flight measurements. Even in doing so, error can be introduced into the data because

hygroscopic materials will start absorbing water as soon as they are exposed to ambient atmosphere. Therefore, even with careful techniques, variations in the weight of a sample from day to day can be significant with respect to the very small changes in mass often associated with low fluence exposures. For this reason is it recommended that weight loss of samples be measured using vacuum dehydrated samples as specified in ASTM E 2089-00 (reference 10).

2.1.2. Uncertainty of Erosion Yield using Mass Loss Technique. Mass loss of polymers as a result of atomic oxygen erosion can be very sensitive providing that an accurate balance is used and that the samples are in the same state of hydration as mentioned above. Because the erosion yield is the volume loss per incident atom, its calculation based on mass loss requires measurements of the change in mass as well as knowledge of the density, the exposed area of the sample (usually using a circular exposure area), for both the test sample as well as the atomic oxygen fluence witness. The resulting erosion yield can then be expressed as

$$E_S = E_K \frac{\left(\Delta M_S D_K^2 \rho_K\right)}{\left(\Delta M_K D_S^2 \rho_S\right)} \tag{4}$$

Where, based on previous shuttle flight experiments:

D_S = *exposed diameter of a circular flight sample, (cm) = 2.065 cm*

D_K = *exposed diameter of a circular flight Kapton witness sample, (cm)*
   = 2.065 cm

Thus the ability to accurately measure the erosion yield of a sample (E_S) using mass loss techniques is dependent upon 4 mass measurements (before and after mass measurements for both the test sample as well as the Kapton fluence witness). The uncertainty of the erosion yield, δE_S, has been calculated by Banks with the assumption that the diameters of the exposed areas for both the Kapton H fluence witness and the test sample are identical.[11] For the current analysis we assume that there is some variability in the exposed diameter of both the Kapton H fluence witness and the test sample.

By propagation of errors, the fractional probable error of the erosion yield of a material, $\delta E_S / E_S$, made by mass loss measurements is given by

$$\frac{\delta E_S}{E_S} = \frac{1}{E_s} \sqrt{\sum_i \left(\frac{\partial E_s}{\partial x_i} \delta x_i\right)^2} \tag{5}$$

Substituting in the variables results in

$$\frac{\delta E_S}{E_S} = \sqrt{\left(\frac{\delta E_K}{E_K}\right)^2 + \left(\frac{\delta \Delta M_S}{\Delta M_S}\right)^2 + \left(\frac{\delta \Delta M_K}{\Delta M_K}\right)^2 + \left(\frac{2\delta D_S}{D_S}\right)^2 + \left(\frac{2\delta D_K}{D_K}\right)^2 + \left(\frac{\delta \rho_S}{\rho_S}\right)^2 + \left(\frac{\delta \rho_K}{\rho_K}\right)^2} \tag{6}$$

Where, based on previous shuttle flight experiments and the assumption that the erosion yields and density of the test polymers are approximately that of Kapton H we have:

δE_K = probable error in erosion yield of Kapton H fluence witness, (cm³/atom)
  = 5 x 10⁻²⁶ cm³/atom

$\delta \Delta M_s$ = probable error in mass loss of the flight sample, (g) = 1.305 x 10⁻⁵ g

$\delta \Delta M_K$ = probable error in mass loss of the Kapton H fluence witness sample, (g)
  = 1.305 x 10⁻⁵ g

$\delta \rho_s$ = probable error in density of flight sample, (g/cm³) = 0.005 g

$\delta \rho_K$ = probable error in density of Kapton H fluence witness sample, (g/cm³)
  = 0.005 g/cm³

δD_s = probable error in exposed diameter of the flight sample, (cm) = 4.23 x 10⁻³ cm

δD_K = probable error in exposed diameter of the Kapton H fluence witness sample, (cm)
  = 4.23 x 10⁻³ cm

Thus, assuming $\delta \Delta M_s = \delta \Delta M_K$, $\delta \rho_K = \delta \rho_s$, and $\delta D_K = \delta D_s$, and combining the above assumptions and substituting for the mass loss, one obtains:

$$\frac{\delta E_S}{E_S} = \sqrt{\left(\frac{\delta E_K}{E_K}\right)^2 + 32\left(\frac{\delta \Delta M_K}{\pi \rho_K D_K^2 E_K F}\right)^2 + 8\left(\frac{\delta D_K}{D_K}\right)^2 + 2\left(\frac{\delta \rho_K}{\rho_K}\right)^2} \tag{7}$$

Figure 2 is a plot of the fractional uncertainty (expressed in terms of percent probable error) in atomic oxygen erosion yield, $\delta E_S / E_S$, as a function of atomic oxygen fluence for the mass loss technique. At atomic oxygen fluences below 2.78 x 10¹⁹ atoms/cm², the percent probable error grows in excess of 5%.
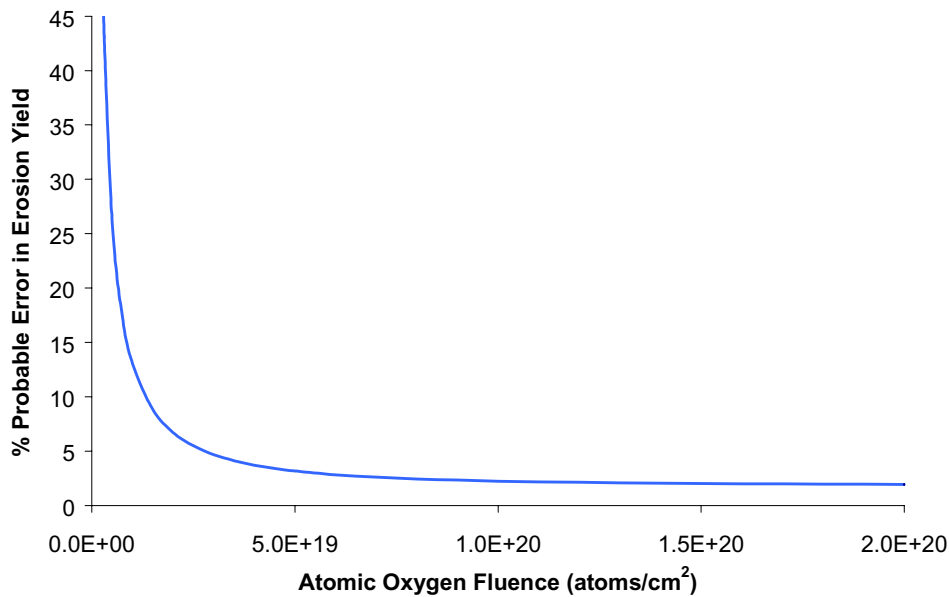

Figure 2. Percent probable error in the atomic oxygen erosion yields as a function of atomic oxygen fluence for the mass loss technique.

2.2. Recession Techniques: Issues and Problems

Recession measurements have been used for erosion yield determination based on erosion depth step-heights. The erosion or recession depth can be measured from a protected surface using profilometry with a stylus profilometer, or with scanning electron microscopy (SEM), optical interferometry or atomic force microscopy.[12] If the surface is protected by a mesh placed over the surface or by applying a protective film onto the surface, the erosion yield, *E*, can be calculated simply through the following equation

$$E = y/F \tag{8}$$

where

$y =$ *step height, or erosion depth (cm)*

For very small erosion depths, techniques for step-height determination such as stylus profilometry, SEM and even optical interferometry are not sensitive enough or have other faults. For example, SEM are not typically set up to obtain accurate erosion depth measurements (Z direction measurements) and making stylus measurements on soft polymers can be problematic. The only technique that can provide accurate very small step-height measurements is AFM. An atomic force microscope can have a lateral resolution of 10-20 Å and sub-angstrom vertical resolution.[13]

2.2.1. Mesh Techniques. Metal meshes such as stainless steel or nickel etched mesh have been used to protect surfaces from atomic oxygen attack resulting in step-height changes in polymers for atomic oxygen erosion yield measurement.[12] The problem with using a mesh technique is that the mesh needs to be very thin and in intimate contact with the polymer to be able to accurately measure the step-height. However it is very difficult to place a thin mesh in intimate contact with the polymer. The quantification of the error associated with the thickness and intimacy of the mesh with respect to the polymer (specifically the height of the mesh surface to the polymer surface) is similar to that reviewed in the section 2.4. And as will be seen, the height plays a critical role in the error of the erosion yield measurements.

2.2.2. Film Techniques. Coatings such as metals, SiO_2, and Al_2O_3 are reported as serving as potential effective masks as long as the coatings are $\geq$ 20 nm thick.[12] The problem with the mask technique is that the thickness of the coating needs to be very accurately known for low fluence exposures and the coating must end cleanly and sharply. That is to say a gradual thinning of the protective coating at its margin (which commonly occurs) will contribute to step-height errors.

2.3. AFM Recession Technique (Intimate Protection & Post-Flight AFM Analysis).

The proposed recession depth technique involves pre-flight protection of the sample surface using isolated intimate contact of small particles. These particles, such as salt crystals or mica powder are applied either by salt spraying or mica dusting resulting in isolated protective

particles. The particles are then removed post-flight (i.e. washing off the salt with distilled water and then nitrogen gas drying) and erosion depth step-height or recession measurements are then obtained using AFM. Specifics about the salt-spraying and mica dusting techniques, and AFM profiling will be discussed in sections 3.1, 3.2 and 3.3, respectively. Figure 3 is an example of how a small protective particle (i.e. salt likely deposited from ocean mist on the launch pad) can protect the underlying polymer from atomic oxygen erosion.
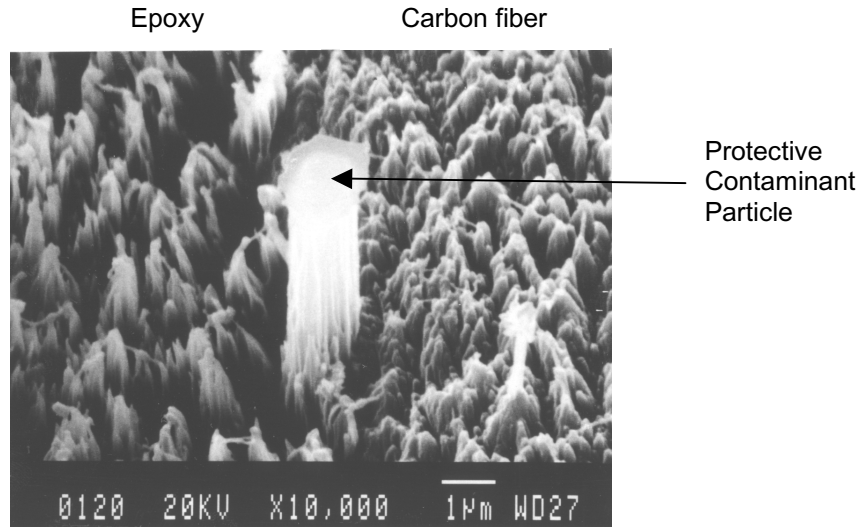

Figure 3. High magnification image of a graphite epoxy composite sample that was flown as part of the Environmental Oxygen Interaction with Materials (EOIM-III) experiment aboard STS-46. This sample was exposed to an atomic oxygen fluence of 2.3 x 10^{20} atoms/cm^2.

2.3.1   Uncertainty of Erosion Yield using AFM Recession Technique.   The sample erosion yield, E_S, calculated by the AFM recession technique in conjunction with the use of the same technique for determining the atomic oxygen fluence based on a Kapton H witness (i.e. recession step height for both the sample and the witness) is given by

$$E_S = E_K \frac{y_S}{y_K}$$

(9)

Where

y_S = *erosion depth of the sample material, (cm)*

y_K = *erosion depth of the Kapton H fluence witness, (cm)*

Thus the fractional uncertainty of the erosion yield, $\delta E_S / E_S$, is given by

$$\frac{\delta E_S}{E_S} = \sqrt{\left(\frac{\delta E_K}{E_K}\right)^2 + \left(\frac{\delta y_S}{y_S}\right)^2 + \left(\frac{\delta y_K}{y_K}\right)^2}$$

(10)

Thus one can see that if one knows the erosion yield of the Kapton H fluence witness well, then the uncertainty in the erosion depths will have a dominant impact on the fractional uncertainty of the erosion yield of the sample. For polymeric materials with erosion yields near that of Kapton H (3.0×10^{-24} cm^3/atom), the resulting fractional uncertainty in erosion yield using this technique is

$$\frac{\delta E_S}{E_S} = \sqrt{\left(\frac{\delta E_K}{E_K}\right)^2 + 2\left(\frac{\delta y_K}{y_K}\right)^2} \qquad (11)$$

Figure 4 shows a schematic diagram of the variables to be considered to calculate the fractional uncertainty in erosion yield using this technique.
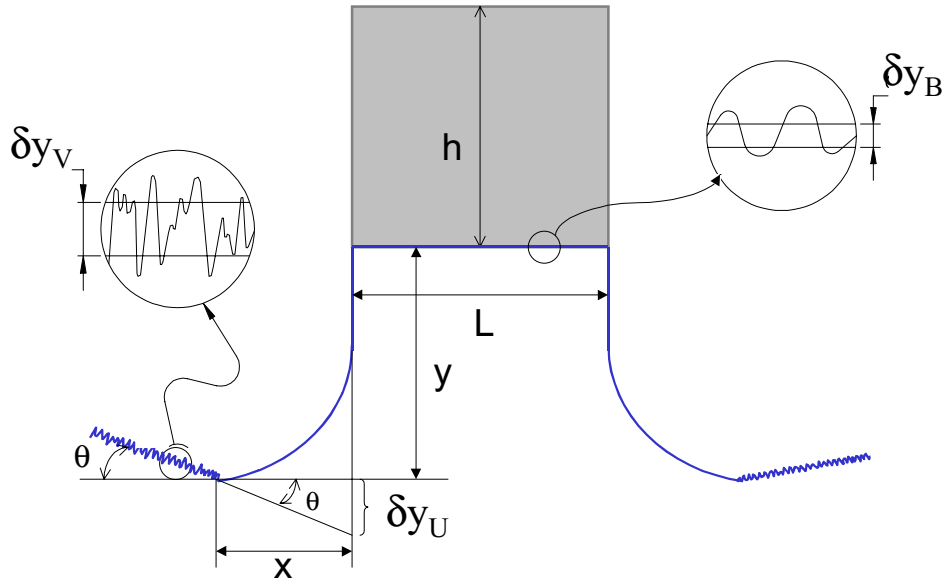

Figure 4. Schematic diagram indicating the various variables associated with the AFM recession depth measurement technique.

As can be seen from figure 4, the error in measurement of the atomic oxygen erosion step height, y, is dependent upon the uncertainty associated with the roughness of the butte formed by the protecting salt crystal, δy_B, the uncertainty associated with the roughness of the atomic oxygen eroded valley, δy_V, and the uncertainty associated with the unevenness or local slope of the valley, δy_U. Thus combining these uncertainties we obtain

$$\delta y = \sqrt{(\delta y_B)^2 + (\delta y_V)^2 + (\delta y_U)^2} \qquad (12)$$

The value for δy_B can be measured using AFM techniques and was found to be 2.31×10^{-8} cm for the smooth side of a pristine Kapton surface.

The value for, δy_V, is dependent upon the square root of the depth of atomic oxygen erosion, y, because roughness is thought to obey Poisson statistics.

Thus the value of δy_V is given by

$$\delta y_V = k_1 \sqrt{y} \qquad (13)$$

Where k_1 is a constant.

Based on the AFM analysis of a salt sprayed Kapton sample exposed to LEO atomic oxygen as part of the Limited Duration Candidate Exposure (LDCE-4) shuttle flight experiment on STS-51, k_1 was found to be 3.947 x 10^{-6}. This sample is described in detail in section 3.3.1.

The value of δy_U, the probable error in y associated with the valley unevenness, is dependent upon the thickness of the atomic oxygen shielding particle, h, the depth of erosion, y, the slope due to the unevenness of the polymer and the fact that even under direct ram atomic oxygen exposure there is an angular distribution of arriving atoms. If we assume that the width of the butte, L, is small enough that the top of the butte can be made level (for mathematical convenience), and if one projects the slope of the valley to the point directly under the edge of the butte, then δy_U is given by

$$\delta y_U = x \tan \theta \qquad (14)$$

Where θ is the angle relative to horizontal of the valley in the region immediately beyond the atomic oxygen penumbra (the region where the fluence of atomic oxygen was partially blocked due to its distribution of arrival angles, see Figure 4).

From AFM measurements of the Kapton LDCE flight sample, θ was found to be 1.28°.

However x is proportional to the distance from the top of the protecting particle to the bottom of the erosion valley. Thus

$$x = k_2 (y + h) \qquad (15)$$

Where k_2 is a constant, which from AFM measurements of the Kapton LDCE-4 flight sample was found to be 0.0698.

Thus combining the equations for the various uncertainties for δy and substituting these into Equation 11 and replacing y with $E_k F$ for polymers with erosion yields near Kapton H results in a fractional uncertainty in erosion yield that is in terms of atomic oxygen fluence and protective particle height. Thus

$$\frac{\delta E_S}{E_S} = \sqrt{\left(\frac{\delta E_K}{E_K}\right)^2 + 2\left(\frac{\delta y_B}{E_K F}\right)^2 + \frac{2k_1^2}{E_K F} + 2\left[k_2\left(1+\frac{h}{E_K F}\right)\tan\theta\right]^2} \tag{16}$$

Figure 5 is a plot of the fractional uncertainty (expressed in terms of percent probable error) of the erosion yield, $\delta E_S / E_S$, as a function of protective particle height for four atomic oxygen fluences. As can be seen from this plot there is a very significant dependence of particle height on the erosion yield uncertainty, particularly for low atomic oxygen fluences. This data shows the importance of having intimate contact with the sample, and for having a thin or very small (if cubic) protective particle for low fluence exposures.   It is clear from this data, that protective mesh techniques are not ideal for erosion yield determination for low fluence missions because they are not in intimate contact, thus resulting in relatively large distances from the top of the mesh to the sample surface (equivalent to a large particle thickness).
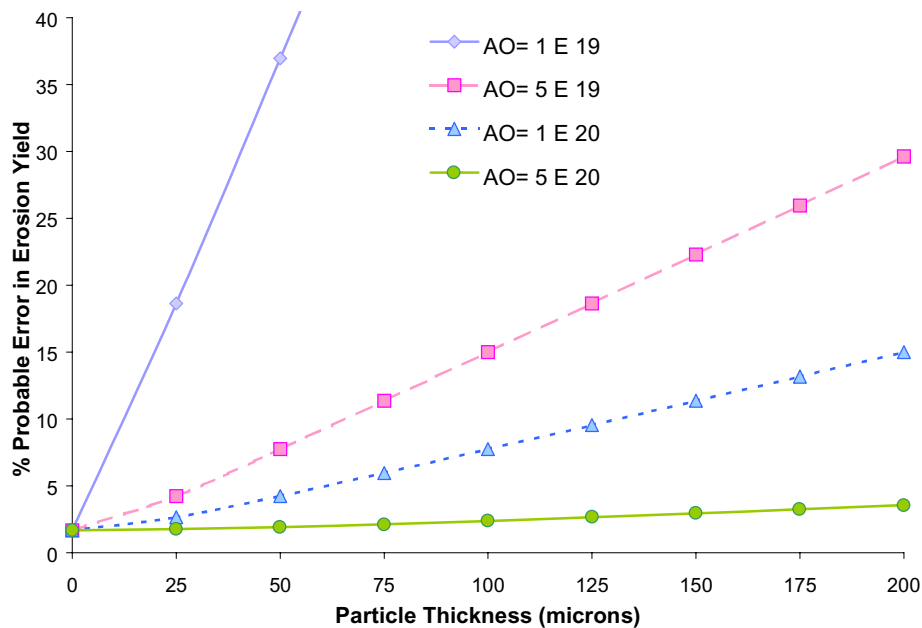

Figure 5. Percent probable error in the atomic oxygen erosion yields as a function of protective particle height for four atomic oxygen (AO) fluences (in atoms/cm^2) for the AFM recession technique.

Figure 6 is a plot of fractional uncertainty (expressed in terms of percent probable error) of the erosion yield, $\delta E_S / E_S$ as a function of atomic oxygen fluence for a protective salt particle 10 microns thick. From the data provided in Figure 6, it is necessary to have an atomic oxygen fluence of at least 1.64 x 10^{19} atoms/cm^2 to obtain percent probable errors of the order of 5% or less for buttes formed by 10 μm thick protective particles.
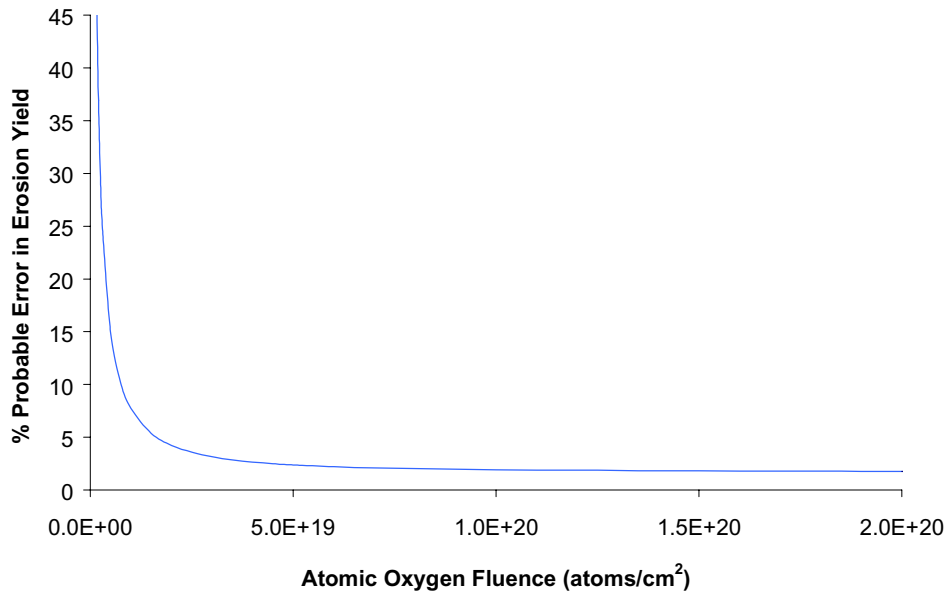
Figure 6. Percent probable error in the atomic oxygen erosion yields as a function of atomic oxygen fluence for 10 μm thick protective salt crystals.

2.4.   Uncertainty Comparisons between Mass Loss and AFM Recession Techniques.

A comparison of erosion depth and mass loss techniques and their associated uncertainties has been evaluated previously by Banks as reported in reference 11. These original results indicate that AFM erosion depth measurements have approximately one half the uncertainty of mass loss measurements for fluences of less than 1×10^{19} atoms/cm^2: 6% probable error for AFM erosion depth technique and 10% for mass loss technique for a fluence of 1×10^{19} atoms/cm^2. However the error analysis in reference 11 did not take into account the uncertainty, δy_U, associated with the unevenness of the valley next to the protected buttes. The results for the new error analyses for the mass loss and AFM recession techniques are compared in Figures 7 and 8. The new analyses indicate a higher error for both of these techniques: 7.74% probable error for recession measurements (using a 10 μm thick protective particle) and 13.1% for mass loss measurements for an atomic oxygen fluence of 1×10^{19} atoms/cm^2. For a fluence of 2×10^{19} atoms/cm^2, the probable error is 6.72% for the mass loss technique and 4.23% for the AFM recession technique (for a 10 μm thick particle). As a reminder, the original mass loss analysis assumed the diameter of the sample and the witness samples were identical, which is no longer assumed in the current mass loss analysis.
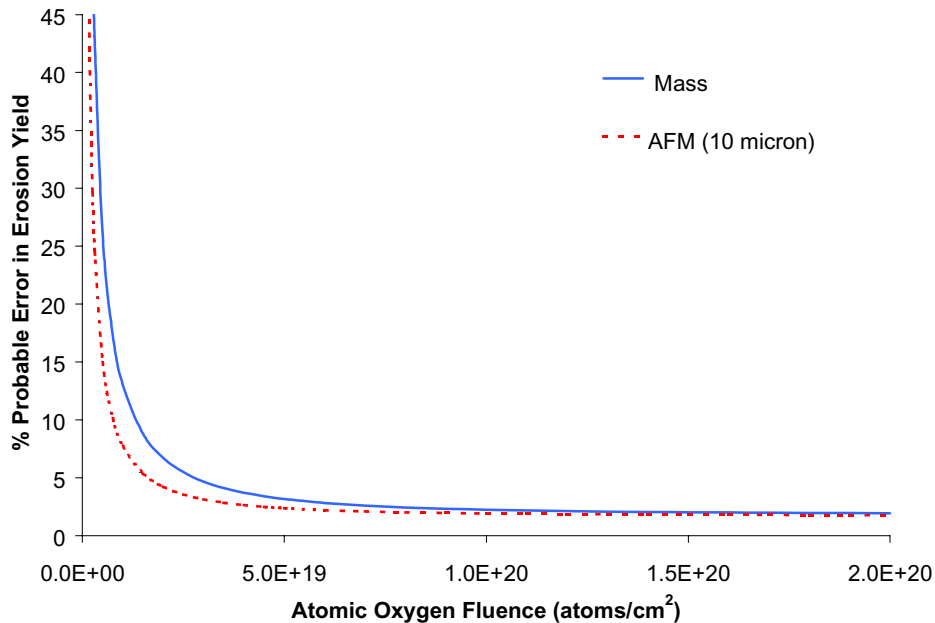
Figure 7. Comparison of the percent probable error in the atomic oxygen erosion yields as a function of atomic oxygen fluence for the mass loss and AFM recession (10 μm particle height) techniques.

As can be seen in Figure 7, for low atomic oxygen fluences (<1 x 10^{20} atoms/cm^2) the AFM recession measurement technique (for a 10 μm thick protective particle) is more sensitive than the mass loss technique. As pointed out above, for a fluence of 1 x 10^{19} atoms/cm^2, the recession uncertainty for a 10 μm thick protective particle is nearly half that of the mass loss uncertainty (7.74% vs. 13.1%, respectively). If we further compare the uncertainty in the AFM recession technique for various protective particle thicknesses as compared to the mass loss technique, as seen in Figure 8, we see that for thick protective particles (specifically >17 μm) the mass loss technique is more accurate, even for low fluences. Specific values have been listed in Table 1 for comparison. These results were somewhat surprising, but understandable as thicker particles produce a much fuzzier step height erosion edge, upon which AFM analyses are dependent on. It should be noted that the variables used in the AFM recession technique uncertainty were obtained from only one flight sample, and are not from a statistical batch of flight data.
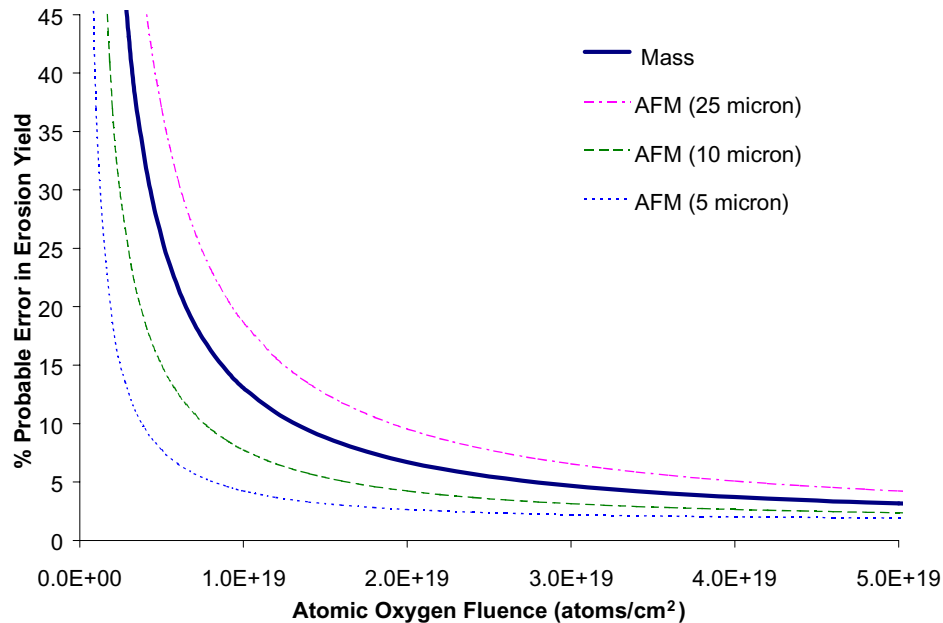
Figure 8. Comparison of the percent probable error in the atomic oxygen erosion yields as a function of atomic oxygen fluence for the mass loss technique and the AFM recession technique for three different protective particle sizes.

As a point of reference for a reasonable goal, a 5% probable error in erosion yield requires an atomic oxygen fluence of 2.78 x 10^{19} atoms/cm^2 for the mass loss technique and 1.64 x 10^{19} atoms/cm^2 for the AFM recession technique using 10 µm thick particles (see Table 1).

Table 1. Probable Error in the Erosion Yield based on Mass Loss and Recession Techniques.

Atomic Oxygen Fluence (atoms/cm^2)	% Probable Error in Erosion Yield			
	Mass Loss	AFM Recession (Particle Height)		
		5 µm	10 µm	25 µm
5.00 x 10^{18}	25.9	7.74	15.0	36.9
1.00 x 10^{19}	13.1	4.23	7.74	18.6
1.64 x 10^{19}	8.11	2.98	**5.00**	11.6
2.78 x 10^{19}	**5.00**	2.27	3.31	7.02
5.00 x 10^{19}	3.17	1.92	2.37	4.23
1.00 x 10^{20}	2.24	1.77	1.92	2.65

3. AFM Recession Measurement Experimental Procedures and Issues

3.1. Salt Spray Procedures and Issues

3.1.1. Salt Spraying and Salt Crystal Variations.   Protective salt particles are applied to the sample substrate by spraying a saturated salt solution using an atomizer. Ideally it is desired to

have a uniform distribution of small cubic crystals. Experiments conducted for the development of a shuttle flight experiment called PEACE (Polymer Erosion And Contamination Experiment)[11] have shown that salt spraying can result in a variety of different salt particles being formed. Examples of these particle types are small or large cubic crystals, oval or asymmetric spherical particles, crystals with salt "rings" around them and even doughnut shaped rings (when the solution is heated). These examples are shown in Figure 9.
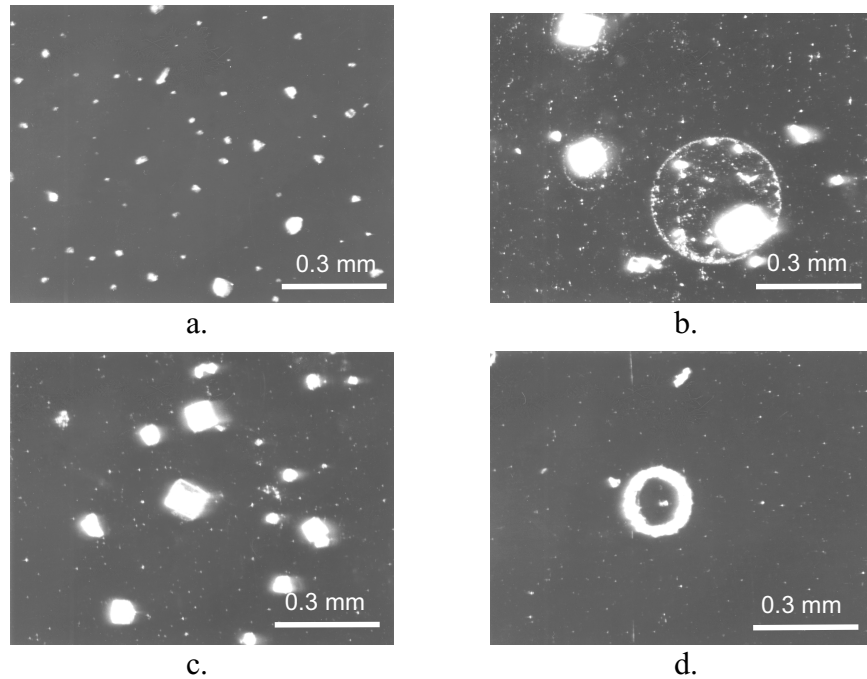

Figure 9. Optical micrographs of different types of salt particles formed on a Kapton HN substrate during salt-spraying: a. small irregular shaped particles, b. salt rings around large (roughly cubic) crystals, c. large cubic and irregular shaped crystals and d. doughnut shapes particles.

3.1.3. Salt-Rings. Of particular concern are the salt rings that are often left around the salt crystals, as shown in Figure 9b. The concern is whether the area within the ring is fully or partially protected from atomic oxygen attack. If the area inside the salt ring is only partially protected, then these crystals can not be used for recession depth analyses. An experiment was conducted to determine if salt-rings would be a problem for analyses using the AFM recession technique. A salt-sprayed Kapton sample was exposed to atomic oxygen in a RF plasma asher for 47 hours (for an effective fluence of approximately 3×10^{20} atoms/cm^2). After atomic oxygen exposure the salt was removed and the sample was coated with a thin conductive film. Then the sample was imaged using a scanning electron microscope (SEM). Figure 10 shows a set of images of one of these salt crystal ring areas before and after atomic oxygen exposure. These tests indicate that the salt ring itself is either fully or somewhat protective of the surface immediately below, but the area within the ring (excluding the salt particle) is eroded to an extent similar to the area outside the ring. This can be seen in Figures 10c and d, where the area adjacent to the protective crystal is eroded to the same depth as the area outside of the salt ring.

Therefore, although salt rings sufficiently distanced from salt particles are usable for obtaining flight data, care needs to be taken when obtaining the erosion depth data to avoid the rings.
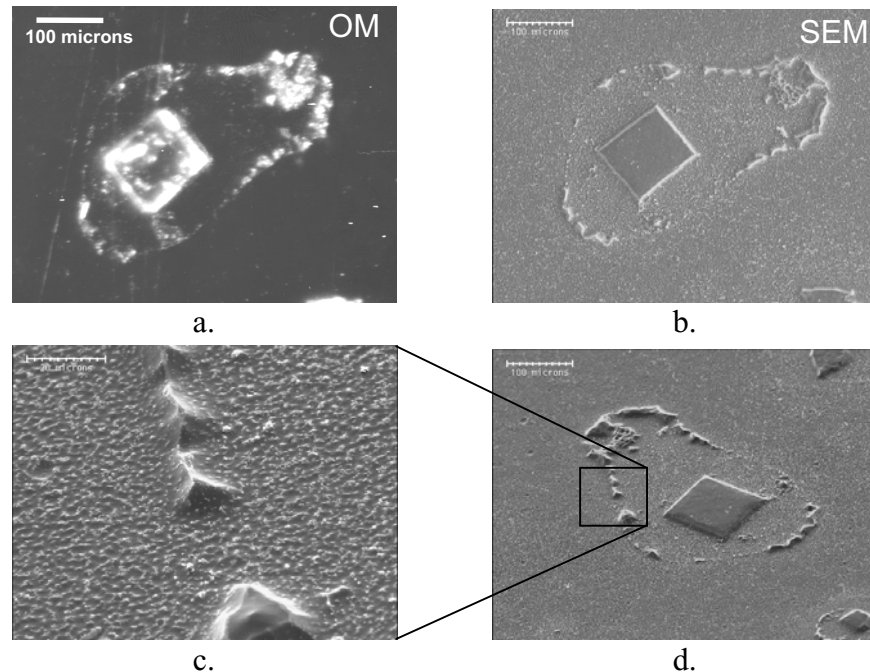

Figure 10. Set of images of a cubic salt crystal surrounded by a salt ring: a. optical micrograph taken prior to atomic oxygen exposure (salt crystal present), b. SEM image taken after atomic oxygen exposure (salt crystal removed), c. close up of the salt ring section indicated in d, d. same image as seen in b at ≈30° tilt angle.

3.1.3. Condensation Issues and Tests. While the shuttle is on the launch pad prior to flight, a potential problem may arise with condensation that may have a negative effect on the protective salt crystals. Prior laboratory tests have shown that the salt crystals on the polymer surfaces act as nucleation sites for condensation, resulting in the salt crystals dissolving with condensation build-up. The resulting salt-water may spread on the sample (or "wet down") depending on the interfacial surface energy (or surface tension) between the three interfaces: the polymer surface and the air, the salt-water and the air, and the salt-water and the polymer. The interfacial surface energy influences the shape of the salt-water bead. If the salt water spreads out as a thin layer on the polymer, many much smaller salt crystals, that are possibly touching, or partially protective, will form as the salt-water drys. This is not desirable, as individual isolated salt particles are needed for the AFM recession measurements. In anticipation of this problem, it is recommended that moisture condensation tests be conducted on the specific polymers prior to characterization using the AFM recession technique. Such tests can be conducted by putting samples in a freezer then removing them to allow purposeful condensation of moisture to accumulate on salt-sprayed samples. The effects of condensation can then be observed using optical microscopy. This test would indicate if a particular polymer would have a problem with condensation, and therefore should be protected using another form of particle such as mica dust.

For the PEACE project, moisture condensation freezer tests were conducted on many different polymer materials. The polymer samples were sprayed with a salt solution, and specific salt crystals were photographed and their positions documented using an optical microscope. The samples were then placed in a freezer for a minimum of 3-4 hour to allow the samples to freeze. After being taken out of the freezer the samples were quickly covered, and then exposed to room temperature air while being viewed with an optical microscope. Photographs were taken during build-up of condensation on the previously documented crystals (to verify that the crystals had dissolved) and also after the salt solution has dried. The pre- and post-freezer pictures were compared and analyzed to determine how condensation affected the salt crystals. An example of a set of micrographs of a freezer test is shown in Figure 11. As can be seen in this series of micrographs, the salt crystals clearly act as nucleation sites for condensation build up. For this particular polymer, ETCFE (ethylene-chlorotrifluoroethylene, also known as Halar), the original salt crystals were cubic whereas the post-freezer (condensation-dried) particles are no longer cubic but more rounded. Also as can be seen in the images in Figure 11 several of particles have moved slightly. These rather rounded salt particles are not ideal, but remain in protective intimate contact, and hence are acceptable.
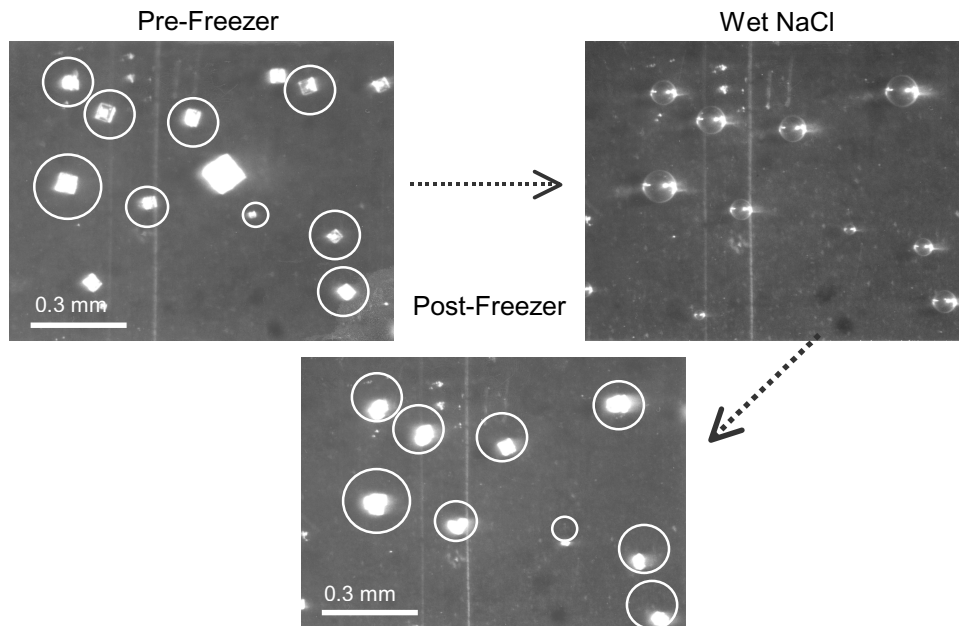

Figure 11. Series of optical micrographs of the polymer ETCFE typical of a freezer test sequence.

3.2. Mica Dusting

For samples that can not be protected with salt particles, such as polymers that dissolve in water or those where the freezer-condensation tests indicate that the dried salt crystals do not provide acceptable protection, other types of protective materials need to be considered. Mica dust is proposed as an alternative protective particle. Mica dust has the advantage of being extremely thin and flat. Experiments have been conducted with mica dusting for the PEACE flight project. A dusting box was built and various tests were conducted to determine good dusting conditions.

Figure 12 is an example of mica dusted Kapton samples. One of the problems encountered with mica dusting was mica clustering due to electrostatic charge build-up on the sample. An example of such clustering is shown in Figure 12a. Figure 12b shows a relatively good distribution of mica particles.

1.67 mm
0.26 mm

a.   b.
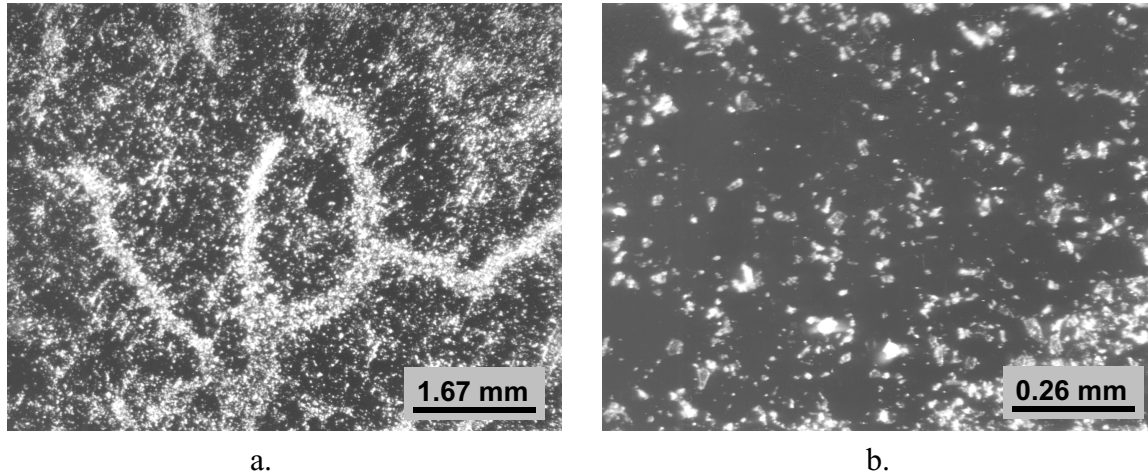
Figure 12. Mica dusted Kapton: a. example of mica clustering due to electro-static charge problem, and b. example of relatively good dust distribution.

Although the use of salt particles has been considered the primary means of providing protection for the AFM recession technique, the error analyses reported in section 2.3.1 indicate that the protective particle height plays a critical role in the erosion yield uncertainty. Therefore, it is recommended that additional tests be conducted to help determine which technique is best over all. Various issues need to be addressed such as determining the ease of mica dust removal (salt is easily removed), determining the capability to produce small salt crystal particles (mica dust is small) and determining how to obtain direct comparisons between salt particle and mica dust height.

3.3.   AFM Procedures and Issues: Contact versus Non-Contact Imaging

An AFM procedure study was conducted to determine which method of AFM data collection, contact versus non-contact, yielded the best estimate of erosion depth. One concern was that contact imaging might produce less accurate results because of flattening of the fine carpet like texture of the eroded area. On the other hand, non-contact imaging (where the cantilevered probe "floats" above the surface) is much more difficult to obtain. An actual flight sample that was prepared for erosion depth measurements and then exposed to a low LEO atomic oxygen fluence on the shuttle was used to obtain contact and non-contact AFM erosion depth data.

3.3.1. Flight Sample. A small (1.9 cm diameter) sample with four different materials (Kapton, Teflon FEP, Teflon AF 1600 and polyphosphazene) was salt-sprayed for AFM erosion depth analysis and flown as part of the Limited Duration Candidate Exposure (LDCE-4) shuttle flight experiment on STS-51, see Figure 13. The LDCE hardware was mounted inside the cargo bay enclosed within a Get Away Special (GAS) canister that was equipped with a motorized door.

The sample was exposed to normal incident ram atomic oxygen for 38 hours (the motorized door was only opened to expose the flight samples to the space environment when the cargo bay was pointed towards the direction of travel (i.e. in the direction of the shuttle's velocity vector)). The salt was washed off post-flight and AFM measurements were made to determine the erosion depth from the salt-protected regions (herein referred to as islands). Because the erosion yield of Kapton is well characterized in the LEO environment (3.0×10^{-24} cm^3/atom), and is therefore used as a witness material in ground-based and flight experiments, the Kapton region was solely concentrated on for this study.
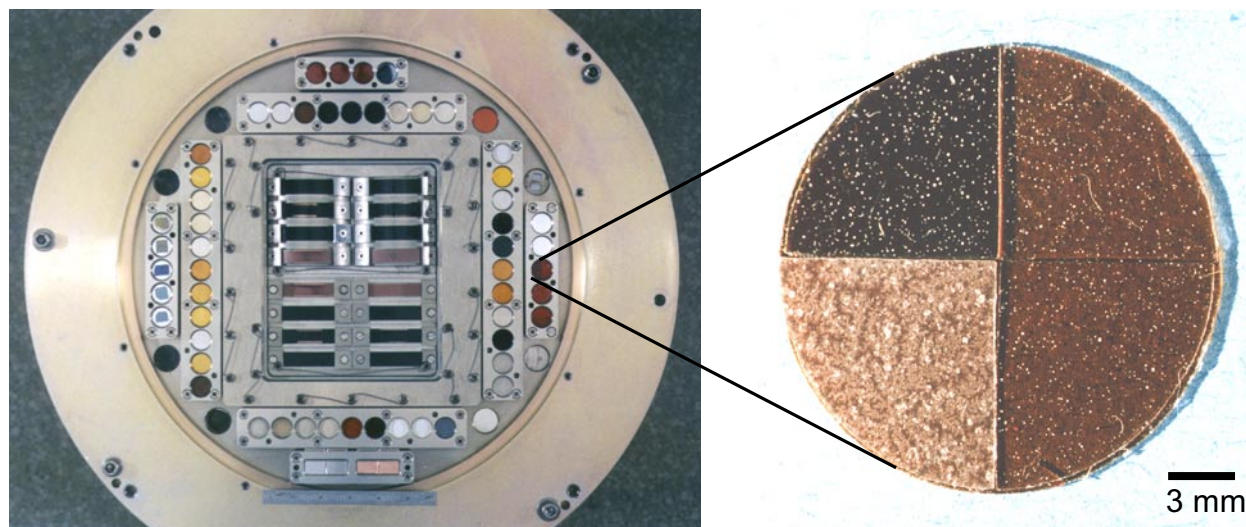

3 mm

Figure 13. Limited Duration Candidate Exposure (LDCE-4) flight hardware and sample prior to flight aboard the shuttle during STS-51.

3.3.2 Atomic Force Microscope Procedures. To obtain measurements an AFM probes the surface of a sample with a sharp tip, a couple of microns long. The tip is located at the free end of a cantilever that is 100 to 200 µm long. Forces between the tip and the sample surface cause the cantilever to bend, or deflect. A detector measures the cantilever deflection as the tip is scanned over the sample, or the sample is scanned under the tip. The measured cantilever deflections allow a computer to generate a map of surface topography.[13]

The flight sample was analyzed using a Park Scientific AutoProbe LS AFM with Park Scientific ProScan 1.3 data acquisition and image processing software. The AFM was equipped with an optical microscope focused on the tip-sample region for approach and island location. The two modes of analysis used were non-contact (NC) mode and contact mode (operated in constant force mode). The AutoProbe LS uses a scanning sample method where the sample is scanned in X, Y and Z directions below the tip.

In constant-force contact mode the tip on the end of the cantilever probe bends or deflects with surface topography. The system then sends a signal to keep the deflection constant by adjusting the position (Z direction) of the sample underneath the stationary cantilever. The changes in sample Z position to maintain a constant deflection of the cantilever provides topographical data,

as the sample is rastered in the x and y directions underneath the cantilever probe. With the cantilever deflection held constant, the total force applied to the sample is constant.[13]

In NC mode the cantilever is driven to oscillate continuously at its resonance frequency. The amplitude of this oscillation changes in response to changes in attractive van der Waals force between the tip and the sample (associated with the changing topography). The NC-AFM system operates to keep the amplitude of oscillation constant, which in turn raises or lowers the sample under the stationary cantilever resulting in topographical information. The spacing between the tip and the sample in for NC-AFM is on the order of tens to hundreds of angstroms.[13]

Four different regions of the Kapton coated region were studied with a total of six different salt-protected islands. On each island, imaging was first carried out in NC-mode and followed by contact mode scans to reduce the possibility of sample damage due to tip-sample contact during contact mode operation. Typical NC imaging parameters included imaging amplitude (cantilever vibration amplitude) of 0.032 μm and a cantilever driving frequency of 370 kHz. Contact mode data were collected at a setpoint (force) of 10 nN. Fairly low scan rates were used for each mode due to the relatively large step height of the islands. Typically, a scan rate of 0.25 lines/sec was used for each 256 line image; a line of data consisted of 256 data points. For each island, several different images of different sizes, from 3 μm x 3 μm to 74 μm x 74 μm, were obtained. All data were corrected for sample tilt (based on flattening the eroded surface only) using a second-order polynomial fit algorithm. A total of 30 different relatively noise-free image pairs were used for the step-height data analysis.

3.3.3. Atomic Force Microscope Results. Figure 14 shows a comparison of images taken in NC mode and contact mode on a typical salt-protected island. The atomic oxygen erosion depth was determined by measuring the vertical (z-direction) change in height from the edge of an island to the eroded surface below. A simple way to make such a measurement would be to take a line profile of the step. However, both the island top and the eroded surface below exhibited some small variation in topography. To average out the effects of such small-scale local variations, step-heights were measured using a line-averaging feature of the Proscan 1.3 imaging analysis software (see Figure 15). Using this feature, one selects a line segment perpendicular to the step edge at the salt-protected/non-protected interface (solid line in figure 15a) and sweeps the line segment through an area parallel to itself along the step to give the region bounded by the dotted line in 15a. A line profile is generated that reflects the average z-value of the swept-through region. One then selects specific points on the line profile for measuring the step height (indicated by the tick marks labeled "0" in the figure). For each pair of images multiple areas were analyzed using this technique.
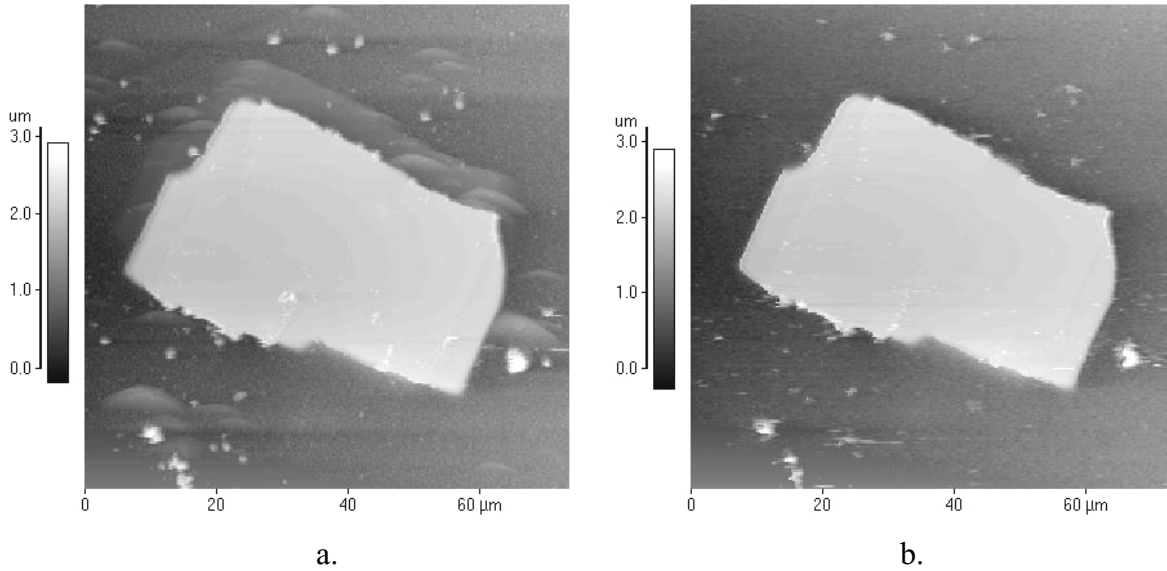
Figure 14. A typical pair of images from one of the salt-protected regions: a. image taken in NC mode, and b. image obtained in contact mode.
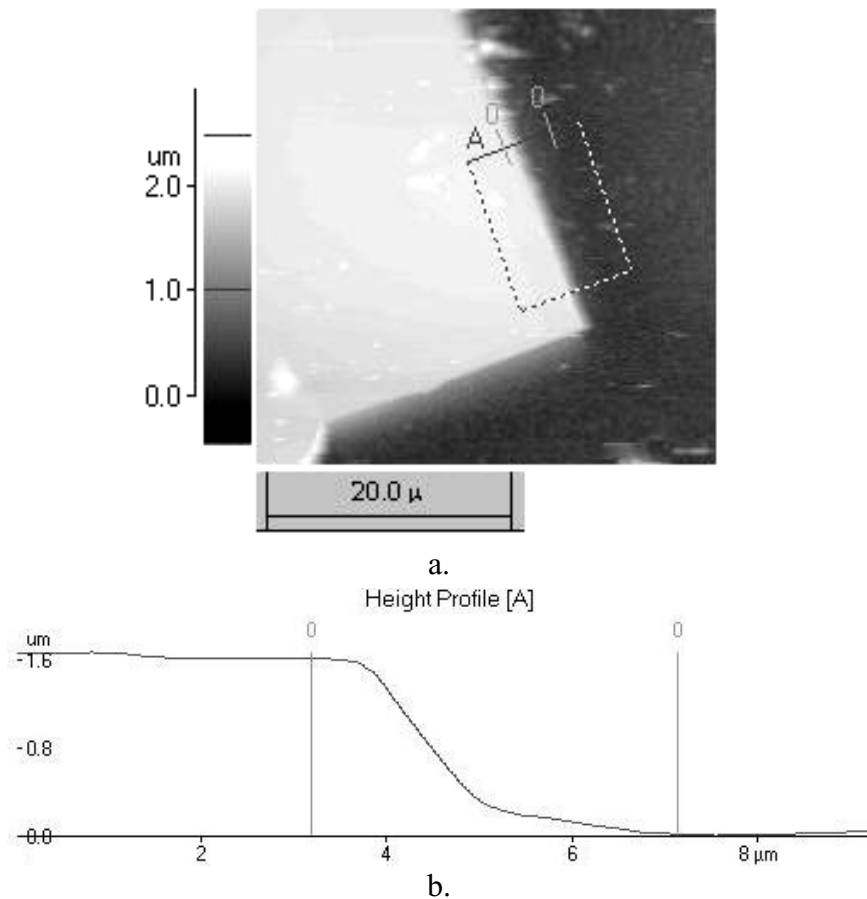

a.

b.

Figure 15. Example of the line averaging technique: a). a sample region in which a line averaging profile has been taken (the solid line segment is perpendicular to the step edge at the salt-protected/non-protected interface), b). The line profile that reflects the average z-value of the swept-through region.

Figure 15.   Example of the line averaging technique: a). a sample region in which a line averaging profile has been taken (the solid line segment is perpendicular to the step edge at the salt-protected/non-protected interface), b). The line profile that reflects the average z-value of the swept-through region.

The results for NC mode and contact mode are provided in Table 2. As can be seen, the results were comparable. The overall average step height was 1.61 µm ± 0.34 µm (standard deviation) using NC mode and 1.47 µm ± 0.13 µm for contact mode. Thus, there is no statistically significant difference between the measured step heights using the two different measurement methods and atomic oxygen erosion depth can be estimated using either AFM mode. Because contact-mode measurements are much easier to make, one can use the technique for atomic oxygen erosion depth measurement without fear of significantly degrading the sample.

Table 2. AFM Data for Non-Contact and Contact Images.

Region	Island #	Height (µm)	
		Non-contact	Contact
NC-1	1 (NC-1-1)	1.448, 1.530	1.411, 1.539
NC-1	1 (NC-1-1)	1.594, 1.721, 1.712	1.539, 1.603, 1.530
NC-1	1 (NC-1-1)	2.185, 2.267, 2.204	1.685, 1.685, 1.430
NC-1	3 (NC-1-2)	2.158, 2.012	1.439, 1.475
NC-1	3 (NC-1-2)	2.012, 2.149	1.402, 1.603
NC-2	4 (NC-2-1)	1.357, 1.348, 1.275	1.348, 1.384, 1.366
NC-2	4 (NC-2-1)	1.229, 1.466, 1.430	1.357, 1.466, 1.484
NC-2	5 (NC-2-2)	1.348, 1.293	1.348, 1.202
NC-2	5 (NC-2-2)	1.229, 1.348, 1.466, 1.466	1.302, 1.439, 1.503, 1.448
NC-3	2 (NC-3-1)	1.639, 1.721, 1.748	1.621, 1.676, 1.703
NC-4	6 (NC-4-1)	1.339, 1.393, 1.156	1.375, 1.457, 1.320
Average		1.608	1.471
STD	+/-	0.338	0.127

4. Additional Comparisons between AFM Recession and Mass Loss Techniques

In addition to the fact that the AFM recession technique can be more accurate for low atomic oxygen fluence exposures, this technique has other desirable advantages as compared to the mass loss technique. One advantage of the AFM recession technique is that no pre-flight data acquisition is necessary. This means that less sample handling is necessary, and it eliminates the additional error introduced in taking sample measurements over a potentially extended period of time (samples often need to be characterized up to a year or more prior to a shuttle mission). Another significant advantage is that very small sample areas can be used. Also, multiple types of polymers can be put together as part of one flight sample (such as the LDCE-4 sample with 4 different polymers on a 1.9 cm diameter sample). This is not possible with mass loss measurements. The disadvantage of the AFM recession technique is that an AFM is necessary, and there is more work involved in the post-flight data analyses.

5. Summary and Conclusions

A recession measurement technique has been developed by GRC using protection of polymer samples with small intimate contact particles, combined with post-flight atomic force microscopy analysis, to obtain accurate erosion yields of polymers exposed to low atomic oxygen fluences. This AFM recession technique has the advantage that very small sample areas can be used to obtain erosion yield data, and multiple polymers can be put together as one flight sample. Error analyses were computed for this technique and for the traditional erosion yield determination technique based on mass loss, and both were highly dependence on atomic oxygen fluence as expected. The recession technique was found to be very dependent on protective particle height in addition to atomic oxygen fluence, and was found to be more accurate than the mass loss technique for protective particles less than 17 μm thick. For example, for a fluence of 1×10^{19} atoms/cm^2, the probable error in the atomic oxygen erosion yield for the AFM recession technique (using a 10 μm thick protective particle) is approximately 60% of the mass loss uncertainty (7.74% vs. 13.1%, respectively). The error analysis results stress the importance of using an intimate contact technique with very small protective particles (if cubic salt crystals are used) or very thin particles such as mica dust.

Specific procedures and issues were addressed for the AFM recession technique including salt spraying, salt crystal variations, potential problems with salt-rings and condensation, and mica dusting. Also addressed were specific AFM procedures. A salt-sprayed sample flown as part of the LDCE-4 shuttle flight experiment was used to study the use of contact versus non-contact mode imaging for determining erosion depth measurements. Analyses indicate that there is no statistically significant difference between the measured step heights using the two different measurement methods and therefore erosion depth can be measured using either AFM mode. Because contact-mode measurements are much easier to make, one can use the contact mode technique for erosion depth measurement without significantly degrading the sample.

The AFM recession depth technique is currently planned to be used to determine the erosion yield of 42 different polymers in the shuttle flight experiment PEACE potentially to be flown in 2002 or 2003. As part of PEACE, identical polymers will be flown and their erosion yields determined using the mass loss technique, so a direct comparison between these two erosion yield techniques will be made.

6. References

1. Banks, B. A., Mirtich, M. J., Sovey, J. S., Nahra, H. and Rutledge, S. K., NASA CP-3109, Vol. 2, 1990, pp. 179-184.
2. *U.S. Standard Atmosphere*, 1976, U.S. Govt. Printing Office, Washington, D.C., 1976, p. 30.
3. Banks, B. A., Rutledge, S. K., Auer, B. M. and DiFilippo, F., *Materials Degradation in Low Earth Orbit (LEO)*, TMS Society, 1990, pp. 15-33.

4. Gregory, J. C., Proceedings of the NASA Workshop on Atomic Oxygen Effects, Nov. 10-11, 1986, JPL 87-14, 1987, pp. 29-30.
5. Stein, B. A. and Pippin, H. G., NASA CP 3134, Part. 2, pp. 617-641.
6. Silverman, E. M., NASA CR 4661, Part 1., August 1995.
7. de Groh, K. K. and Banks, B. B., J. Spacecraft & Rockets, Vol. 31, No. 4, 1994, pp. 656-664.
8. de Groh, K. K., Dever, J. A., McCollum, T. A., Rodriguez, E., Burke, C. and Terlep J. A., Solar Engineering 1992, Vol.2, ASME, pp. 775-782.
9. Banks, B. A., de Groh, K. K., Auer, B. M. and Gebauer, L., NASA CP 3257, 1994, pp.143-158.
10. ASTM E 2089-00 Standard Practices for Ground Laboratory Atomic Oxygen Interaction Evaluation of Materials for Space Applications, Annual Book of ASTM Standards, 2000.
11. Banks, B. A., de Groh K. K., Baney-Barton, E., Sechkar, E. A., Hunt, P., Willoughby, A., Bemer, M., Hope, S., Koo, J., Kaminski, C. and Youngstrom, E., NASA TM-1999-209180, May 1999.
12. Minton, T. K., JPL Publication 95-17, Version 2, 1995.
13. Howland, R. and Benatar, L., *A Practical Guide to Scanning Probe Microscopy,* Park Scientific Instruments, 1996.

REPORT DOCUMENTATION PAGE

1. AGENCY USE ONLY (Leave blank)	2. REPORT DATE	3. REPORT TYPE AND DATES COVERED
	December 2001	Technical Memorandum

4. TITLE AND SUBTITLE

A Sensitive Technique Using Atomic Force Microscopy to Measure the Low Earth Orbit Atomic Oxygen Erosion of Polymers

5. FUNDING NUMBERS

WU–755–1A–13–00

6. AUTHOR(S)

Kim K. de Groh, Bruce A. Banks, Gregory W. Clark, Anne M. Hammerstrom, Erica E. Youngstrom, Carolyn Kaminski, Elizabeth S. Fine, and Laura M. Marx

7. PERFORMING ORGANIZATION NAME(S) AND ADDRESS(ES)

National Aeronautics and Space Administration
John H. Glenn Research Center at Lewis Field
Cleveland, Ohio 44135–3191

8. PERFORMING ORGANIZATION REPORT NUMBER

E–13162

9. SPONSORING/MONITORING AGENCY NAME(S) AND ADDRESS(ES)

National Aeronautics and Space Administration
Washington, DC 20546–0001

10. SPONSORING/MONITORING AGENCY REPORT NUMBER

NASA TM—2001-211346

11. SUPPLEMENTARY NOTES

12a. DISTRIBUTION/AVAILABILITY STATEMENT

Unclassified - Unlimited
Subject Categories: 18 and 27   Distribution: Nonstandard

Available electronically at http://gltrs.grc.nasa.gov/GLTRS

This publication is available from the NASA Center for AeroSpace Information, 301–621–0390.

12b. DISTRIBUTION CODE

13. ABSTRACT (Maximum 200 words)

Polymers such as polyimide Kapton and Teflon FEP (fluorinated ethylene propylene) are commonly used spacecraft materials due to their desirable properties such as flexibility, low density, and in the case of FEP low solar absorptance and high thermal emittance. Polymers on the exterior of spacecraft in the low Earth orbit (LEO) environment are exposed to energetic atomic oxygen. Atomic oxygen erosion of polymers occurs in LEO and is a threat to spacecraft durability. It is therefore important to understand the atomic oxygen erosion yield (E, the volume loss per incident oxygen atom) of polymers being considered in spacecraft design. Because long-term space exposure data is rare and very costly, short-term exposures such as on the shuttle are often relied upon for atomic oxygen erosion determination. The most common technique for determining E is through mass loss measurements. For limited duration exposure experiments, such as shuttle experiments, the atomic oxygen fluence is often so small that mass loss measurements can not produce acceptable uncertainties. Therefore, a recession measurement technique has been developed using selective protection of polymer samples, combined with postflight atomic force microscopy (AFM) analysis, to obtain accurate erosion yields of polymers exposed to low atomic oxygen fluences. This paper discusses the procedures used for this recession depth technique along with relevant characterization issues. In particular, a polymer is salt-sprayed prior to flight, then the salt is washed off postflight and AFM is used to determine the erosion depth from the protected plateau. A small sample was salt-sprayed for AFM erosion depth analysis and flown as part of the Limited Duration Candidate Exposure (LDCE-4, -5) shuttle flight experiment on STS-51. This sample was used to study issues such as use of contact versus non-contact mode imaging for determining recession depth measurements. Error analyses were conducted and the percent probable error in the erosion yield when obtained by the mass loss and recession depth techniques has been compared. The recession depth technique is planned to be used to determine the erosion yield of 42 different polymers in the shuttle flight experiment PEACE (Polymer Erosion And Contamination Experiment) planned to fly in 2002 or 2003.

14. SUBJECT TERMS

Atomic oxygen; Low Earth orbit durability; Polymer erosion; Atomic force microscopy; Space flight experiment

15. NUMBER OF PAGES

30

16. PRICE CODE

17. SECURITY CLASSIFICATION OF REPORT	18. SECURITY CLASSIFICATION OF THIS PAGE	19. SECURITY CLASSIFICATION OF ABSTRACT	20. LIMITATION OF ABSTRACT
Unclassified	Unclassified	Unclassified	